What controls aerosol sensitivity in clouds formed by homogeneous freezing?

Jennifer E. Kay[1] and Robert Wood[2]

[1] National Center for Atmospheric Research, Boulder, CO, jenkay@ucar.edu, ph: 303-497-1730

[2] Department of Atmospheric Sciences, University of Washington, Seattle, WA

Abstract:

Understanding the sensitivity of cloud properties to aerosols is essential to credible climate prediction. In warm clouds, increasing aerosol number concentrations (N_a) increases hydrometeor concentrations and for a fixed water content, produces brighter clouds that cool the climate (Twomey, 1974). Does a similar effect exist for cold clouds? In this paper, we define a dimensionless parameter R that predicts and explains N_a sensitivity in clouds formed by homogeneous freezing. Using R, we explain why N_a sensitivity increases dramatically with ice deposition coefficients (α_i) << 0.1, and why N_a sensitivity increases as vertical velocity increases, temperature decreases, N_a decreases, and aerosol size decreases. We combine existing observations with modeling to suggest that $\alpha_i > 0.1$ in the atmosphere. We conclude that N_a changes may only affect cold clouds that form at large vertical velocities, or at low temperatures found in the tropical upper troposphere.

1. Introduction

Human emissions of greenhouse gases and aerosol particles are changing the Earth's atmosphere. In addition to their direct effects, changes in greenhouse gas and aerosol concentrations may also have indirect effects on the climate system. Clouds cover 60% of the Earth's surface and play a large role in regulating the Earth's radiation budget. If appreciable changes in cloud cover and/or properties result from changing atmospheric conditions, the Earth's climate will be altered. Yet, cloud processes and cloud responses to changing atmospheric conditions remain among the least well understood elements of our climate system.

Twomey (1974) described the first indirect effect of increasing aerosol concentrations (N_a [m^{-3}]) on clouds: For a fixed water content, the drop number concentration and brightness of warm clouds increases. Current estimates of the global Twomey effect for warm clouds, i.e., the change to the top-of-atmosphere (TOA) radiative forcing due to increases in atmospheric N_a since pre-industrial times, range from -0.5 to -1.9 Wm^{-2} (Lohmann and Feichter, 2005).

In contrast, modeling studies have shown the number of ice crystals (N_i [m^{-3}]) resulting from homogeneous freezing is relatively insensitive to upper tropospheric N_a (e.g., Jensen and Toon (1994), DeMott et al. (1997), Kärcher and Lohmann (2002a,b), Kärcher and Ström (2003)). In other words, these studies imply a cold cloud aerosol sensitivity (η_a) << 1 where:

$$\eta_a \equiv \frac{d(\ln N_i)}{d\ln(N_a)} \quad (1)$$

Observations show a positive, but weak correlation, between N_i and N_a during cold cloud formation (Siefert et al., 2004). If η_a is larger than these studies suggest, an increase in anthropogenic N_a in the lower troposphere will increase upper tropospheric N_a and cold cloud N_i. For a fixed water content, increasing N_i will increase cold cloud albedos and alter radiative fluxes. Therefore, it is important to understand the atmospheric conditions under which cold clouds are sensitive to changes in N_a.

In this paper, we investigate the physical factors that determine η_a in cold clouds formed by homogeneous freezing. Although aerosols that serve as ice nuclei can alter cold cloud properties, for simplicity we do not consider the impact of heterogeneous freezing on cold cloud aerosol indirect effects. In Section 2, we demonstrate with an explicit parcel model (Kay et al., 2006) that a simple analytical expression explains the dependence of η_a upon thermodynamic factors including vertical velocity (w [m s^{-1}]) and co-varying temperature (T [°C]) and pressure (P [mb]), and microphysical factors including N_a, hydrated aerosol radius (r_a [m]), and the ice deposition coefficient or mass accommodation coefficient (α_i). In Section 3, we discuss the implications of our results for the atmosphere. In Section 4, we summarize our results and provide suggestions for future work.

Our work builds on the analytical results of Kärcher and Lohmann (2002a,b) (hereafter KL). KL found that N_i is primarily controlled thermodynamically rather than microphysically, with a strong dependence upon w. However, KL neglected two important microphysical factors. First, KL did not explore the consequences of current uncertainty in α_i, i.e., the fraction of impinging water vapor molecules that are incorporated into an ice crystal lattice (Pruppacher and Klett, 1997). KL assumed α_i=1 in their analysis, but laboratory measurements of α_i vary from 0.006 to 1 (e.g., Haynes et al. (1992), Magee et al. (2006)). In addition, KL did not treat explicitly the potential for the N_a to become depleted by freezing, a factor which is important when N_i are limited by N_a.

2. What determines η_a ?

For simplicity, we consider cold cloud formation during ascent at constant w. The supersaturation with respect to ice (S_i) increases during ascent and at the beginning of freezing (time t=0 [s]) the homogeneous freezing rate (J_{hom} [m^{-3} s^{-1}]), a logarithmically increasing function of S_i reaches a threshold value (J_o [m^{-3} s^{-1}]). Freezing stops at a later time (t_{freeze} [s]) when vapor deposition on newly formed ice crystals causes S_i to decrease and J_{hom} to decrease below J_o. Given this physical picture of cloud formation, the N_i generated in a homogeneous freezing event can be approximated as:

$$N_i = \int_0^{t_{freeze}} J_{\hom}(S_i(t)) \frac{4}{3} \pi r_a(t)^3 N_a(t) dt \quad (2)$$

With this physical picture of cold cloud formation, η_a depends on many thermodynamic and microphysical variables. We hypothesize that η_a can be predicted by the timescale ratio:

$$R \equiv \frac{\tau_{growth}}{\tau_{lift}} \quad (3)$$

where τ_{lift} is the timescale for increase of S_i via ascent (seconds), and τ_{growth} is a timescale for growth of newly nucleated ice crystals by vapor deposition (seconds). Note: Because ice crystal growth results from vapor deposition, τ_{growth} is also a timescale for the drawdown of S_i.

For R >> 1, ice crystal growth is relatively slow and η_a approaches 1 whereas for R << 1, ice crystal growth is relatively fast and η_a approaches 0.

To evaluate if R can quantitatively predict η_a, analytical expressions for τ_{lift} and τ_{growth} are required. In an analytical analysis based on Eq. (2) and KL, we define τ_{lift} and τ_{growth} as follows:

$$\tau_{lift} = [Q_1 w]^{-1} \quad (4)$$

$$\text{with } Q_1 = \frac{\Gamma}{T}\left(\left(\frac{L_s(S_i+1)}{R_v T}\right) - \frac{5}{2}\right)$$

where Q_1 is a thermodynamic constant, Γ=0.0097 K m^{-1} is a reference lapse rate, L_s=2.834*10^6 J kg^{-1} is the latent heat of sublimation, and R_v=461 J $K^{-1}kg^{-1}$ is the gas constant for water vapor.

$$\tau_{growth} = [(KN_a)^{2/3}(S_i D_v^*)]^{-1} \quad (5)$$

with $K = \sqrt{2(\rho_{sat-i}\rho_i)}$

and $D_v^* = \dfrac{D_v}{\dfrac{r_a}{r_a+\lambda} + \dfrac{D_v}{r_a\alpha_i}\sqrt{\dfrac{2\pi M_w}{R_{ideal}T}}} = \dfrac{D_v}{\dfrac{r_a}{r_a+\lambda} + \dfrac{\lambda}{\alpha_i r_a}}$

where K is a constant, ρ_{sat-i} is the saturation vapor density with respect to ice (kg m^{-3}), ρ_i=900 kg m^{-3} is the density of ice, D_v* is the modified vapor diffusivity (m^2 s^{-1}) (Eq. 13-14 in Pruppacher and Klett (1997)) which includes impedances to growth due to vapor diffusivity and surface processes but neglects the relatively small thermal impedance to growth, D_v is the vapor diffusivity (m^2 s^{-1}) (Eq. 13-3 in Pruppacher and Klett (1997)), λ is the molecular mean free path (m) (Eq. 16.20 in Jacobson (1999)), M_w= 0.018015 kg $mole^{-1}$ is the molecular weight of water, R_{ideal}=8.3145 J $K^{-1}mole^{-1}$ is the ideal gas constant.

By calculating τ_{lift} and τ_{growth} in parcel model experiments (Table 1), we evaluate if η_a can be predicted by R alone. In all cases, we calculated R using the parcel model output at the timestep before freezing begins.

To introduce our parcel model experiments, we first show an experiment in which we only vary α_i (Figure 1). Decreasing α_i increases R by increasing τ_{growth} without affecting τ_{lift}. Indeed, the increase in S_i and J_{hom} resulting from long τ_{growth} is why small α_i lead to large N_i (Gierens et al., 2003). The α_i lifting experiment reveals the dramatic effect of R on the sensitivity of N_i to N_a and on the drawdown of S_i. When efficient growth is assumed (R<<1, α_i > 0.1, blue curves Figure 1), J_{hom} and S_i are quickly reduced by ice crystal growth, and N_i is not sensitive to N_a. In contrast, with inefficient growth (α_i <<0.1, R>>1, red curves Figure 1), J_{hom} and S_i reach large values and the sensitivity of N_i to N_a increases. Surprisingly, the reduction in S_i when α_i=0.01 is faster than when α_i = 1. This counter-intuitive result is explained as follows: When α_i decreases, individual particles grow inefficiently, but N_i and the total surface area dramatically increase.

Although the α_i lifting experiment revealed that there are complex relationships between η_a and atmospheric variables, our parcel model runs suggest η_a can be predicted by R alone (Figure 2a). When multiple parcel model experiments are plotted on one R vs. η_a graph (Figure 2, panel A), they

collapse onto a single line. In other words, one can predict changes in η_a by evaluating the effect of changing atmospheric conditions on R (Eq. 3).

Using a sensitivity test approach, we explored the influence of plausible variations in thermodynamic (w, T, P) and microphysical (α_i, r_a) variables on η_a and R (Figure 2b-d). Through R, we can understand the physical basis for the influence of these parameters on η_a. η_a increases with w because large w result in small τ_{lift}. With $\alpha_i > 0.1$, η_a is always small; however when $\alpha_i < 0.1$, τ_{growth} increases and η_a increases dramatically. η_a increases dramatically when T << -70 °C because low T increases τ_{growth}. Finally, variations in r_a have only a limited influence on η_a. η_a increases slightly as r_a decreases, because for a fixed N_a, small r_a result in long τ_{growth}.

3. Implications for the atmosphere

When α_i <0.1, plausible variations in α_i can dramatically change η_a, and alter the sensitivity of η_a to variations in other microphysical and thermodynamic variables. The influence of α_i on τ_{growth} increases at low α_i because D_v* does not depend directly on α_i, but on $\frac{\lambda}{\alpha_i r_a}$ (see Eq. 5). When $\frac{\lambda}{\alpha_i r_a}$ is small, the precise value of α_i is unimportant because diffusive impediments to growth are more important than surface impediments to growth. Reviews of laboratory measurements at cold cloud temperatures suggest that α_i for small ice crystals could be as low as 0.001 and as high as 1 (Haynes et al., 1992); recent laboratory measurements found α_i=0.006 (Magee et al., 2006). α_i may be a function of ice crystal size and of chemical composition, so it may not be easy to extrapolate laboratory measurements for the atmosphere. Never-the-less, given the sensitivity of η_a to α_i when α_i <0.1, discrepancies between α_i measurements must be resolved.

Fortunately, existing observations can be used to constrain the α_i of small ice crystals in the atmosphere. In general, observed N_i (0.001-10 cm^{-3} (e.g., Mace et al. (2001), Kärcher and Ström (2003)) rarely approach observed N_a (10-500 cm^{-3} (e.g., Rogers et al, (1998), Minikin et al. (2003)). These observations suggest that η_a rarely approaches 1 and α_i are rarely less than 0.1. The INCA field campaign (Kärcher and Ström, 2003) provides a unique opportunity to constrain α_i. Using INCA measurements, we require α_i =~0.1 to simultaneously match the mean N_i, N_a, T, and w in lifting parcel model experiments (Table 2). With α_i =0.006 (Magee et al., 2006), modeled N_i were orders of magnitude larger than INCA-observed N_i. If present, shattering of ice crystals by aircraft probes (e.g., Field et al

(2006)) would reduce observed N_i and increase the α_i required to match INCA-observed values with parcel modeling experiments.

Assuming α_i=0.1 in the atmosphere, cold clouds primarily form in a regime where $\eta_a << 1$ (Figure 3). In other words, the N_i resulting from homogeneous freezing is generally thermodynamically-limited, not aerosol-limited. This outcome agrees with Hoyle et al. (2005), Kärcher and Ström, (2003), and Kay et al. (2006), who all found that atmospheric N_i are primarily controlled by w. With α_i=0.1, our modeling results do suggest there are conditions under which N_i does depend on N_a. First, η_a increases at very large w (approximately w > 100 cm s^{-1} when T=-50 C and α_i=0.1) Second, there is a significant increase in η_a at low T, such as those that would be found in the tropical upper tropopause. Finally, η_a increases as N_a decreases, which can be important at high w or low T.

4. Summary and Discussion

In this study, we used analytical analysis, parcel modeling, and observations to understand the sensitivity of clouds produced by homogeneous freezing to changes in aerosols (η_a - Eq. 1). Our primary findings were:

- The dependence of η_a on a large number of microphysical and thermodynamic variables can be explained and predicted using a single timescale ratio, R (Eq. 3).
- In modeling sensitivity experiments, η_a increases dramatically when $\alpha_i < 0.1$, but also when w increases, T decreases. N_a decreases, or r_a decreases.
- Using existing observations and simple modeling, we suggest small ice crystal $\alpha_i \geq 0.1$ in the atmosphere. As a consequence, η_a is small under most atmospheric conditions, but may increase at large w (w > 100 cm s^{-1}) and at low T (T< -70 °C).

Does a effect similar to the Twomey effect exist for cold clouds? We conclude that for most cold clouds, the answer is no. However, our work suggests that η_a increases at large w and at low T.

We recommend that future studies investigate the implications of this study for clouds forming at low T. Hoyle et al. (2005) proposed that co-varying T and P decreases have competing effects on ice crystal growth rates, and as a result, the N_i generated by homogeneous freezing does not depend on T. In contrast, our modeling results suggest the balancing of T and P effects is not universal and that τ_{growth}, η_a, and N_i increase at low T. Also, because our analyses suggest $\alpha_i \geq 0.1$ in the atmosphere, our work suggests low α_i are an unlikely explanation for atmospheric observations of large persistent S_i (Peter et al.,

2006). Simultaneous observations of N_a and N_i at low T could be used to estimate atmospheric α_i and to evaluate the dependence of η_a on T presented in this study.

Acknowledgments: JEK was supported by NSF-ATM-02-1147 and by the Office of Biological and Environmental Research of the U.S. Department of Energy under contract DE-AC06-76RL01830 to the Pacific Northwest National Laboratory as part of the Atmospheric Radiation Measurement Program. The authors both thank Dr. Marcia Baker for her encouragement and her contributions to this work.

References

DeMott, P. J., D. C. Rogers, and S. M. Kreidenweis (1997), The susceptibility of ice formation in upper tropospheric clouds to insoluble aerosol components, *J. Geophys. Res.*, 102(D16), 19,575-19,584.

Field, P. R., A. J. Heymsfield, and A. Bansemer (2006), Shattering and particle interarrival times measured by optical array probes in ice clouds, *Journal of Atmospheric and Oceanic Technology*, 23(2), 1,357–1,371.

Gierens, K. M., M. Monier, and J. Gayet (2003), The deposition coefficient and its role for cirrus clouds, *J. Geophys. Res.*, 108 (D2), 4069, doi:10.1029/2001JD001558.

Haynes, D. R., N. J. Tro, and S. M. George (1992), Condensation and evaporation of H20 on ice surfaces, *J. Phys. Chem.*, 96, 8,502-8,509.

Hoyle, C. R., B. P. Luo, and T. Peter (2005), The origin of high ice crystal number densities in cirrus clouds, *J. Atmos. Sci.*, 62(7), 2,568-2,579.

Jacobson, M. Z. (1999), *Fundamentals of Atmospheric Modeling*, 656 pp., Cambridge University Press, New York.

Jensen, E. J. and O. B. Toon (1994), Ice freezing in the upper troposphere: sensitivity to aerosol number density, temperature and cooling rate, *Geophys. Res. Lett.*, 21 (18), 2,019-2,022.

Kay, J. E., Baker, M., and D. Hegg (2006), Microphysical and dynamical controls on cirrus cloud optical depth distributions, *J. Geophys. Res.*, 111, D24205, doi:10.1029/2005JD006916.

Kärcher, B., and U. Lohmann (2002), A parameterization of cirrus cloud formation: Homogeneous freezing of supercooled aerosols, *J. Geophys. Res*, 107(D2), 4010, doi:10.1029/2001JD000470.

Kärcher, B., and U. Lohmann (2002), A parameterization of cirrus cloud formation: Homogeneous freezing including effects of aerosols size, *J. Geophys. Res*, 107(D23), 4698, doi:10.1029/2001JD001429.

Kärcher, B. and J. Ström (2003), The roles of dynamical variability and aerosols in cirrus

cloud formation, *Atmos. Chem. Phys.*, 3, 823-838.

Koop, T., B. Luo, A. Tslas, and T. Peter (2000), Water activity as the determinant for homogeneous ice nucleation in aqueous solutions, *Nature*, 406, 611-614.

Lohmann, U. and J. Feichter (2005), Global indirect aerosols effects: a review, *Atmos. Chem. Phys.*, 5, 715-737.

Mace, G. G., E. E. Clothiaux, and T. P. Ackerman (2001), The composite characteristics of cirrus clouds: bulk properties revealed by one year of continuous cloud radar data, *J. Clim.*, 14, 2185-2203.

Magee, N., A. M. Moyle, and D. Lamb (2006), Experimental determination of the deposition coefficient of small cirrus-like ice crystals near −50°C, *Geophys. Res. Lett.*, 33, L17813, doi:10.1029/2006GL026665.

Minikin, A., A. Petzold , J. Strom, R. Krejci, M. Seifert, P. van Velthoven, H. Schlayer, and U. Schumann (2003), Aircraft observations of the upper tropospherice fine particle aerosol in the Northern and Southern Hemispheres at mid latitudes, *Geophys. Res. Lett.*, 30(10), 1503, doi:10.1029/2002GL016458.

Peter, T., C. Marcolli, P. Spichtinger, T. Corti, M. B. Baker, and T. Koop (2006), When dry air is too humid, *Science*, 314, 1,399-1,402.

Pruppacher, H. R. and J. D. Klett (1997), *Microphysics of Clouds and Precipitation*, 2nd ed., 954 pp., Kluwer Academic Publishers, Boston.

Rogers, D. C., P. J. DeMott, S. M. Kredenweis, and Y. Chen (1998), Measurements of ice nucleating aerosols during SUCCESS, *Geophys. Res. Lett.*, 25:9, 1383-1386.

Seifert, M., J. Ström, R. Krejci, A. Minikin, A. Petzold, J.-F. Gayet, H. Schlager, H. Ziereis, U. Schumann, and J. Ovarlez (2004). Aerosol-cirrus interactions: A number based phenomenon at all?, *Atmos. Chem. Phys., 4, 293–305*.

Twomey, S. A. (1974), Pollution and the planetary albedo, *Atmos. Env.*, 8, 1251-1256.

Figures

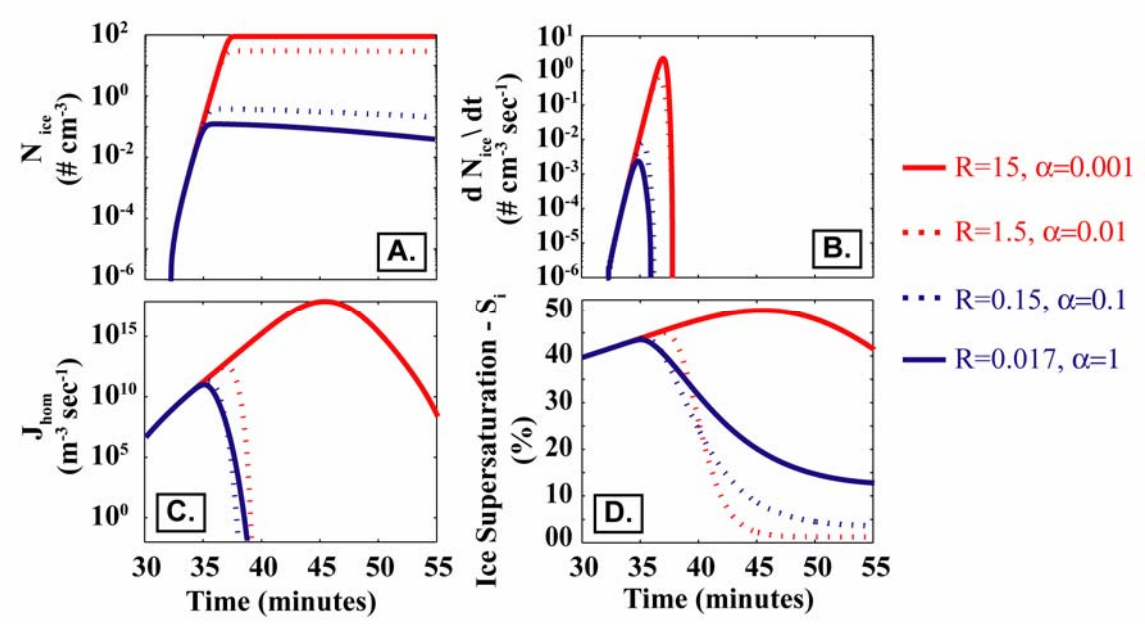

Figure 1. Time series of parcel model lifting experiments (Table 1) with w = 10 cm s^{-1}, T_0 = -50 C, P_0 = 250 mb, N_a=100 cm^{-3}, and r_a=0.2 μm.

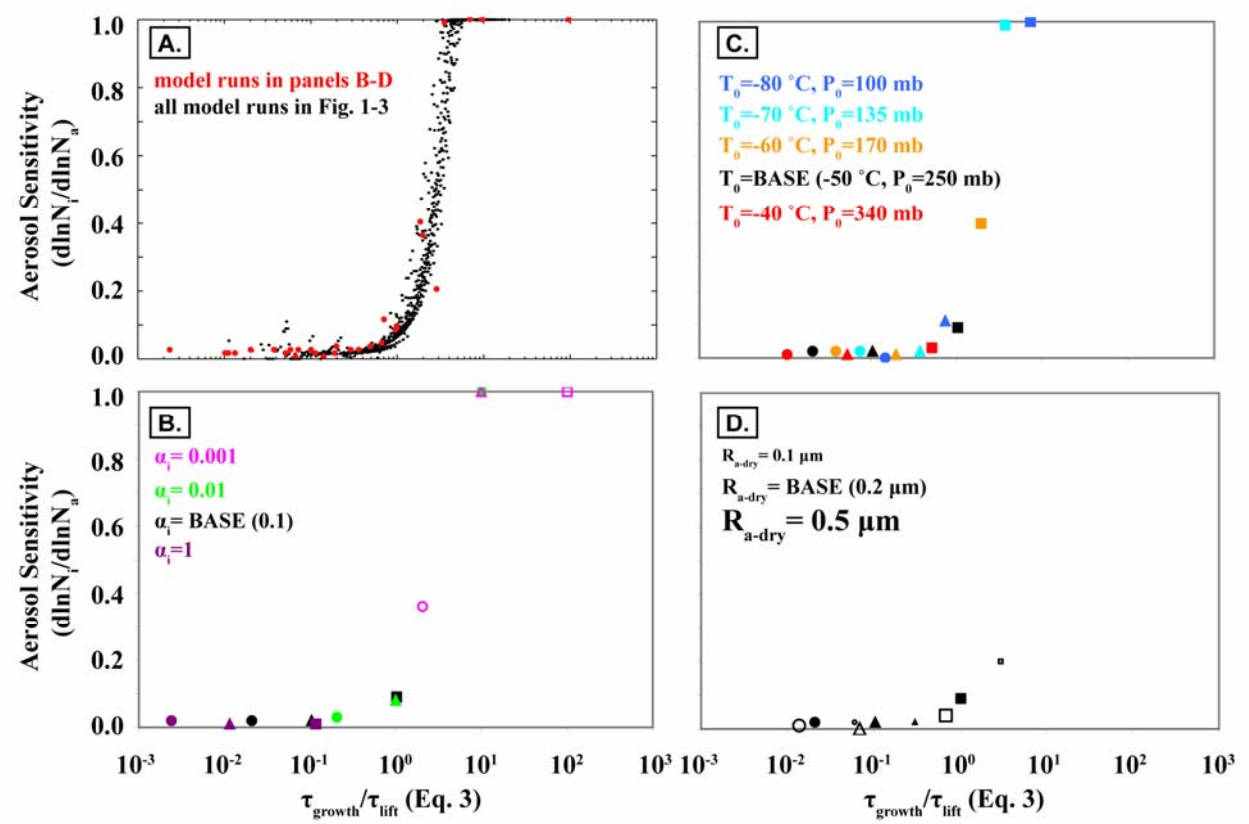

Figure 2. Aerosol sensitivity vs. R for all parcel model runs (panel A) and for a sensitivity test with a range of α_i (panel B), T_0 (panel C) and $r_{a\text{-}dry}$ (panel D). For panels B-D: 1) circles w=2 cm s^{-1}, diamonds w=10 cm s^{-1}, and squares=100 cm s^{-1}. 2) Aerosol sensitivity was calculated using the change in N_i from model runs with N_a=100 cm^{-3} and N_a=500 cm^{-3} (see Eq. 1). 3) Unless otherwise indicated, values are base values: T_0 = -50 °C, P_0 = 250 mb, and r_a=0.2 µm.

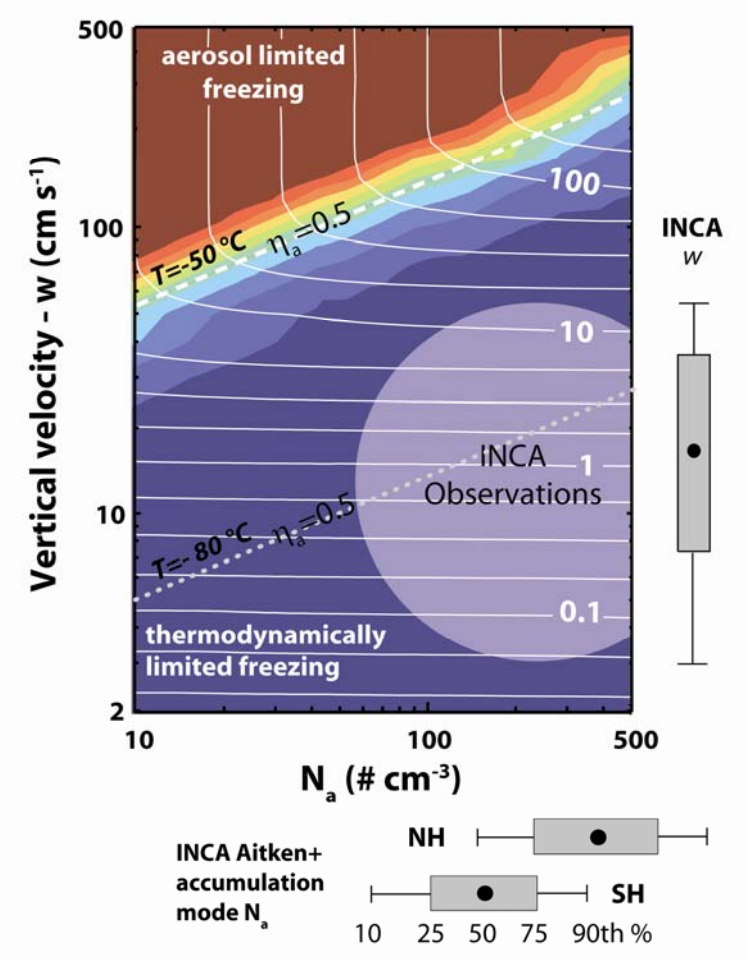

Figure 3. Maximum N_i contoured as a function of vertical velocity (w) and aerosol number concentration (N_a) from the parcel model lifting experiments with α_i=0.1, T_0 = -50 °C, P_0 = 250 mb, and r_a=0.2 μm. Colors indicate the aerosol sensitivity parameter η_a (Eq. 1) in increments of 0.1 from 0 (deep blue) to 1 (deep red). The dashed line shows the boundary (η_a=0.5) between the thermodynamically limited nucleation regime (η_a=0) and the aerosol-limited nucleation regime (η_a=1). The dotted line shows the η_a=0.5 line for the case where T=-80 °C and P_0=100 mb. Plotted w and N_a ranges are from the INCA field campaign (values taken from Kärcher and Ström (2003) and Minikin et al. (2003)).

Tables:

Table 1. Parcel model description and configuration used for this study. In all model runs, α_i does not depend on ice crystal size.

Parcel model description	Model configuration
• description and validation in Kay et al. (2006) • binned ice microphysics (300 bins) • aerosol activation using Köhler curve, 1 aerosol bin, sulfuric acid aerosol with a dry weight of 10^{-16} kg • saturation vapor pressures e_s and es_{ice} from Murphy and Koop (2005)	• parcel lifted at a constant vertical velocity (w) • homogeneous nucleation (Koop et al., 2000) only • ice crystal fallout included with a parcel depth=100 m

Table 2. INCA observations (Kärcher and Ström, 2003) and parcel model predicted N_i. Parcel model N_i are found from constant lifting experiments (Table 1) with INCA-observed w, T, and N_a, and P_0 = 250 mb. In order to match the observed N_i, α_i values of 0.057 and 0.13 were required for the Scotland and Chile observations respectively.

	INCA Observations (Kärcher and Ström, 2003)				**Parcel Model N_i (# cm^{-3})**			
	w (cm s^{-1})	T (ºC)	N_a (# cm^{-3})	N_i (# cm^{-3})	α_i = 1	α_i = 0.1	α_i= 0.01	α_i= 0.006
Scotland	26.2	-48.3	300	5.3	0.5	2.3	102.8	212.6
Chile	23	-46.8	110	1.1	0.4	1.4	61.3	102.7